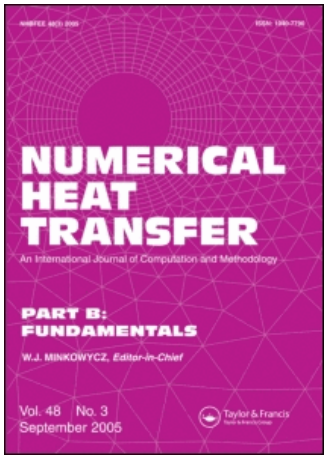

Numerical Heat Transfer, Part B: Fundamentals
An International Journal of Computation and Methodology
Publication details, including instructions for authors and subscription information:
http://www.informaworld.com/smpp/title~content=t713723316

Spectral Element Method with Adaptive Artificial Diffusion for Solving the Radiative Transfer Equation

J. M. Zhao [a]; L. H. Liu [a]
[a] School of Energy Science and Engineering, Harbin Institute of Technology, Harbin, People's Republic of China

Online Publication Date: 01 June 2008

To cite this Article: Zhao, J. M. and Liu, L. H. (2008) 'Spectral Element Method with Adaptive Artificial Diffusion for Solving the Radiative Transfer Equation', Numerical Heat Transfer, Part B: Fundamentals, 53:6, 536 — 554

To link to this article: DOI: 10.1080/10407790802035117
URL: http://dx.doi.org/10.1080/10407790802035117

Numerical Heat Transfer, Part B, 53: 536–554, 2008

ISSN: 1040-7790 print/1521-0626 online
DOI: 10.1080/10407790802035117

Taylor & Francis
Taylor & Francis Group

SPECTRAL ELEMENT METHOD WITH ADAPTIVE ARTIFICIAL DIFFUSION FOR SOLVING THE RADIATIVE TRANSFER EQUATION

J. M. Zhao and L. H. Liu
School of Energy Science and Engineering, Harbin Institute of Technology, Harbin, People's Republic of China

An adaptive isotropically artificial diffusion (AISO) scheme is developed for the spectral element method to mitigate the ray effects encountered in the solution of radiative transfer problems. By considering the coupled manner of ray effects and false scattering, the artificial diffusion coefficient is determined heuristically from both local angular discretization scale and local spatial discretization scale. The scheme is easily and efficiently implemented under the spectral or finite-element method framework. The performance of various artificial diffusion schemes is studied and compared. The streamwise artificial diffusion schemes are only responsible for stabilization of strong convection-induced instability, while the isotropically artificial diffusion scheme shows very good performance in mitigating the "wiggles" in both low- and high-order spatial approximation. Numerical experiments show that the spectral element method with the AISO scheme is stable, high-order-accurate, and effective for solving radiative transfer in simple and complex geometries, and also robust for mitigating ray effects of various origins.

INTRODUCTION

Numerical solutions of the radiative transfer equation (RTE) in participating media require considerable effort for most practical systems. In recent years, the methods based on the discretization of the radiative transfer equation, such as the discrete-ordinates method (DOM) [1], the finite-volume method (FVM) [2–4], and the finite-element method (FEM) [5, 6], have received considerable attention owing to their good compromise among accuracy, flexibility, and moderate computational requirements. Some recent developments include the discontinuous finite element method [7, 8], the spectral or *hp* finite-element method [9, 10], and the discontinuous spectral element method [11], which have shown very good performance. However, former studies show that two kinds of numerical error exist in these methods during the solution of the RTE, namely, ray effects and false scattering, which set critical

Received 21 August 2007; accepted 21 February 2008.
Support of this work by the National Nature Science Foundation of China (50425619) is gratefully acknowledged.
Address correspondence to L. H. Liu, School of Energy Science and Engineering, Harbin Institute of Technology, 92 West Dazhi Street, Harbin 150001, People's Republic of China. E-mail: lhliu@hit.edu.cn

NOMENCLATURE

C	adjustment parameter defined in Eq. (17)	V	solution domain
h_a	local angular discretization scale	x, y, z	Cartesian coordinates
h_s	local spatial discretization scale	α	artificial diffusion coefficient
$\mathbf{H}$	matrix defined by Eq. (9)	β	extinction coefficient
I	radiative intensity, $W/m^2\,sr$	ε_w	wall emissivity
I_b	black-body radiative intensity, $W/m^2\,sr$	κ_a	absorption coefficient, m^{-1}
$\mathbf{K}$	matrix defined in Eq. (9)	κ_s	scattering coefficient, m^{-1}
L	side length, operator defined by Eq. (2)	σ	Stefan-Boltzmann constant, $W/m^2\,K^4$
$\mathbf{n}_w$	unit outward normal vector	τ_L	optical thickness
N_{sol}	total number of solution nodes	ϕ	nodal basis function
N_θ, N_φ	discretization number of polar and azimuth angles	Φ	scattering phase function
p	polynomial order	ω	scattering albedo
q	radiative heat flux, W/m^2	Ω, Ω'	vector of radiation direction
$\mathbf{r}$	spatial coordinates vector	**Subscripts**	
R	radius	i, j	spatial solution node index
S	source function defined by Eq. (3)	w	value at wall
T	temperature, K	**Superscripts**	
		m	the mth angular direction

limitations on the application of these methods. The ray effects are known to be attributed to the angular discretization, while the false scattering is attributed to spatial discretization. Furthermore, the influence of ray effects and false scattering may not be simply taken as independent; they also interact with each other. The false scattering can be overcome by high-order spatial discretization, while the higher-order spatial approximation tends to exaggerate the ray effects. The interaction process of these errors has not been well understood.

The ray effects and the false scattering encountered in the solution of the RTE by the DOM and the FVM have been studied by several researchers [12–15]. Because the ray effects can cause unrealistic "wiggles" in the results and even totally spoil the solution, as compared with false scattering, it can be considered a dominant error in many cases. Recently, several studies have focused on the mitigation of ray effects. Ramankutty and Crosbie [16] developed a modified DOM (MDOM) to solve the radiative transfer in semitransparent media. The MDOM successfully mitigates the ray effects caused by strong nonuniformity (or sharp gradients) of boundary thermal loading. In the MDOM, the radiative intensity is decomposed into a direct component that accounts for the radiative bundle originating directly from the wall and a diffuse component that accounts for the radiative bundle originating from the media, in which the direct component is solved analytically, while the diffuse component is solved by the DOM. However, the MDOM cannot mitigate the ray effects caused by strong nonuniformity of media temperature. Based on a similar principle as the MDOM, while using a different decomposition of the radiative intensity, Coelho [13, 17] proposed a new, improved MDOM (NMDOM), which can mitigate the ray effects caused both by strong nonuniformity of boundary loading and of media

temperature. Though the MDOM and the NMDOM can successfully mitigate the ray effects encountered in the DOM, they have obvious drawbacks. The principle of the MDOM or the NMDOM requires that the radiative intensity be decomposed into a direct component and a diffuse component, in which the direct component has to be solved analytically or by a numerical method that does not suffer from ray effects, while the diffuse component is solved by the DOM. As a result, the solution process of the MDOM is rather complex and difficult to implement compared to the standard DOM and FVM. To develop a general approach that can efficiently and effectively mitigate the ray effects encountered in the numerical methods for solution of the RTE still requires much effort.

The spectral element method combines the competitive advantages of the high-order spectral method, i.e., the *p*-convergence property, and the finite-element method, i.e., the flexibility to deal with complex domains and offering *h*-convergence property. Recent study on the spectral element method for the solution of radiative transfer shows that the higher-order spatial approximation is very effective and efficient [10, 11]. Higher-order approximation brings little false scattering, and solution with very few numbers of elements can give accurate results. However, the spectral element method still suffers from some stability problems. One of the causes of instability is the convection-dominated nature of the RTE [18]. Another important cause of instability is the ray effects, in which insufficient angular discretization will spoil the results with "wiggles". Until recently, little work has been done on the mitigation of ray effects encountered in using the spectral element method to solve the RTE.

In this article, an adaptive, isotropically artificial diffusion (AISO) scheme is developed for the spectral element method to mitigate the ray effects encountered in the solution of radiative transfer problems. By considering the compensate manner of ray effects and false scattering, an artificial diffusion coefficient is determined from both the local angular discretization scale and the local spatial discretization scale. The performance of various artificial diffusion schemes is studied and compared. Four test examples are considered to verify the formulation presented.

MATHEMATICAL FORMULATION

Discrete-Ordinates Equation of Radiative Transfer

The discrete-ordinates equation of radiative transfer in an enclosure filled with participating gray media can be written as

$$L^m[I^m] = S^m(\mathbf{r}) \tag{1}$$

where the linear operator L^m and the source term function $S^m(\mathbf{r})$ are defined respectively as

$$L^m[I^m] = \mathbf{\Omega}^m \cdot \nabla I^m(\mathbf{r}) + \beta I^m(\mathbf{r}) \tag{2}$$

$$S^m(\mathbf{r}) = \kappa_a I_b(\mathbf{r}) + \frac{\kappa_s}{4\pi} \sum_{m'=1}^{M} I^{m'}(\mathbf{r})\, \Phi(\mathbf{\Omega}^m, \mathbf{\Omega}^{m'})\, w^{m'} \tag{3}$$

For the opaque and diffuse boundary, the boundary conditions are given as

$$I_w^m = \varepsilon_w I_{bw} + \frac{1-\varepsilon_w}{\pi} \sum_{\mathbf{n}_w \cdot \Omega^{m'} > 0} I_w^{m'} |\mathbf{n}_w \cdot \mathbf{\Omega}^{m'}| \qquad w^{m'} \mathbf{\Omega}^m \cdot \mathbf{n}_w < 0 \tag{4}$$

where $\mathbf{\Omega}^m$ is the discrete direction vector, β is the extinction coefficient, κ_a and κ_s are the absorption and scattering coefficients, respectively, Φ is the scattering phase function, $\mathbf{n}_w$ is the unit outward normal vector of the wall, ε_w is the wall emissivity, and $w^{m'}$ is the weight of direction $\mathbf{\Omega}^{m'}$ for angular quadrature. The discrete ordinates equation (1) is in a form as a convection-dominated equation [19]. As demonstrated in [11, 18], the convection term may cause nonphysical oscillatory of solutions for radiative transfer problems if no special stability treatment is adapted.

Besides the stability problem caused by the convection-dominated property of the RTE, another important cause of instability is the ray effects which is attribute to angular discretization. In the following sections of the paper, various stability schemes are studied for the spectral element method to overcome these problems.

Artificial Diffusion Schemes for Spectral Element method

The spectral element method can be considered a special kind of finite-element method. The difference is that, in the spectral element method, the nodal basis function $\phi_i(\mathbf{r})$ is constructed on each element by orthogonal polynomial expansion. The unknown radiative intensity can be approximated by a nodal basis function with Kronecker delta property as

$$I^m(\mathbf{r}) \simeq \sum_{i=1}^{N_{\text{sol}}} I_i^m \phi_i(\mathbf{r}) \tag{5}$$

where ϕ_i is the nodal basis function, I_i^m denotes radiative intensity of direction $\mathbf{\Omega}^m$ at solution nodes i, and N_{sol} is the total number of solution nodes. In this article, Chebyshev polynomial expansion is used to build the basis function. Details on building the global nodal basis function are given in [10].

Like the upwind scheme for the finite-difference or finite-volume method, additional artificial diffusion (numerical diffusion) is essential to stabilize the spectral element method. Here two kinds of scheme that bring different modes of artificial diffusion are considered, namely, schemes belonging to the streamwise upwind strategy and a scheme that brings isotropically artificial diffusion.

Streamwise Upwind Strategy

A Streamwise upwind strategy is often taken to stabilize the spectral element method in the solution of convection-dominated equations, including a group of schemes, such as the streamline upwind (SU) scheme [20], the streamline upwind Petrov-Galerkin (SUPG) scheme [20], and the Galerkin least-square (GLS) scheme [21]. More generally, the least-square (LS) scheme can be seen as a special kind of GLS scheme under the condition that the upwind factor is selected to be sufficient

large. In this section, the streamwise upwind strategy is applied to stabilize the radiative transfer equation. Substituting Eq. (5) into Eq. (1) and using the weighted-residual approach yields

$$\sum_{i=1}^{N_{\text{sol}}} I_i^m \left\{ \int_V [\mathbf{\Omega}^m \cdot \nabla \phi_i(\mathbf{r})] W_j(\mathbf{r})\, dV + \int_V [\beta\, \phi_i(\mathbf{r})] W_j\, dV \right\} = \int_V S^m(\mathbf{r})\, W_j(\mathbf{r})\, dV \quad (6)$$

where $W_j(\mathbf{r})$ is the weight function. The weight function W_j is selected as ϕ_j for the Galerkin scheme and $L^m[\phi_j]$ for the LS scheme. As for the convection-type equation given by Eq. (1), a modified weight function different from that used in the Galerkin method is used to obtain various streamwise upwind schemes, namely,

$$W_j = \phi_j + \alpha P[\phi_j] \quad (7)$$

where α is an artificial diffusion coefficient or upwind factor and P is a convection operator. Similar to the upwind schemes used in finite-difference methods, the streamwise upwind schemes for the spectral or finite-element method brings additional diffusion to stabilize the convection-dominated problem, and the artificial diffusion coefficient α characterizes the amount of additional artificial diffusion added. Different upwind schemes can be obtained by taking different P. For example, taking $P = \mathbf{\Omega}^m \cdot \nabla$ and making the weight function W_j impose only on the convection term, namely, the first term of Eq. (6), the SU scheme is obtained; taking $P = \mathbf{\Omega}^m \cdot \nabla$, the SUPG scheme is obtained; and taking $P = L^m$, the GLS scheme is obtained. Equation (6) can be written in matrix form as

$$\mathbf{K}^m \mathbf{I}^m = \mathbf{H}^m \quad (8)$$

where matrices $\mathbf{K}^m$ and $\mathbf{H}^m$ are defined respectively as

$$K_{ji}^m = \int_V (\mathbf{\Omega}^m \cdot \nabla \phi_i) W_j\, dV + \int_V (\beta \phi_i) W_j\, dV \quad (9a)$$

$$H_j^m = \int_V S^m W_j\, dV \quad (9b)$$

Isotropically Artificial Diffusion

Another kind of artificial diffusion scheme is the isotropically artificial diffusion scheme (ISO). The ISO scheme is similar to the viscous finite-difference scheme, namely, by directly adding an isotropically viscous term in the original convection equation, and then the modified equation is discretized by a central difference scheme. As for the spectral or finite-element method, the Galerkin approach is applied. The modified equation with added isotropically artificial diffusion term is written as

$$\mathbf{\Omega}^m \cdot \nabla I^m + \beta I^m = S^m + \alpha \nabla^2 I^m \quad (10)$$

Assuming the artificially diffusion diminishes along the boundary, Eq. (10) is discretized by the Galerkin approach as

$$\sum_{i=1}^{N_{\text{sol}}} I_i^m \left[\int_V (\mathbf{\Omega}^m \cdot \nabla \phi_i + \beta \phi_i) \phi_j \, dV + \alpha \int_V \nabla \phi_i \cdot \nabla \phi_j \, dV \right] = \int_V S^m W_j \, dV \tag{11}$$

Equation (11) can be reformed into matrix form as Eq. (8); here matrices $\mathbf{K}^m$ and $\mathbf{H}^m$ are defined respectively as

$$K_{ji}^m = \int_V (\mathbf{\Omega}^m \cdot \nabla \phi_i + \beta \phi_i) \phi_j \, dV + \alpha \int_V \nabla \phi_i \cdot \nabla \phi_j \, dV \tag{12a}$$

$$H_j^m = \int_V S^m \phi_j \, dV \tag{12b}$$

Adaptive Determination of the Artificial Diffusion Coefficient

Because the artificial diffusion coefficient is responsible for the stability and accuracy of the discretization, its determination is very important. A large value of α will bring an excessive amount of artificial diffusion, which will result in large false scattering, while a small value of α cannot ensure stability. The experiences of many researchers has showed that the stability of methods for solving Eq. (1) relies on both angular and spatial discretization schemes. As a result, the determination of α needs to take into account the influence of both angular and spatial discretization. In this section, the artificial diffusion coefficient is determined heuristically based on knowledge of the property of the discrete ordinates equation.

As a start, consider a general convection diffusion equation given by

$$\mathbf{v} \cdot \nabla u - \alpha \nabla^2 u = f \tag{13}$$

It is well known that the stability condition of Eq. (13) for a central difference scheme or finite-element method can be written as

$$\alpha \geq \frac{1}{2} |\mathbf{v}| h_s \tag{14}$$

where h_s denotes the local spatial discretization length scale. Here $|\mathbf{v}| = |\mathbf{\Omega}| \leq 1$ for the radiative transfer equation. This stability condition shows that the essential artificial diffusion coefficient α is related to h_s as $\alpha \geq C' h_s$, where C' is a constant with $C' < 1$. By considering the coupled interaction of spatial discretization and angular discretization for the radiative transfer equation, especially in the case of ray effects, the stability of the method should be related to the local angular discretization scale h_a. The optimum value of α should decrease with a decrease of h_s and h_a. When $h_a \gg h_s$, the solution error is governed by angular discretization, and the value of α can be considered to be governed by h_a. When $h_s \gg h_a$, the optimum value of α can be considered to be governed by h_s.

Based on the above qualitative analysis, here the artificial diffusion coefficient is assumed to be in a form

$$\alpha(h_a, h_s) = b_1 h_a + b_2 h_s^{p+1} \tag{15}$$

where b_1 and b_2 are two positive constants and p is the order of polynomial approximation for the spectral or finite-element method. Equation (15) simply assumes a linear relation between α and h_a and h_s^{p+1}. The term h_s^{p+1} takes into account the order of polynomial approximation by considering that the artificial diffusion should decrease considerably with increase of polynomial order p. Equation (15) can be rewritten as

$$\alpha(h_a, h_s) = (b_1 + b_2)\left[\frac{b_1}{(b_1 + b_2)} h_a + \frac{b_2}{(b_1 + b_2)} h_s^{p+1}\right] \tag{16}$$

Furthermore, the artificial diffusion coefficient can be reintroduced in a form as

$$\alpha(h_a, h_s) = C h_a + (1 - C) h_s^{p+1} \tag{17}$$

where $C \in [0, 1]$ is considered a balancing parameter for angular and spatial discretization scale. The artificial diffusion coefficient given by Eq. (17) varies adaptively with local spatial discretization scale h_s and angular discretization scale h_a. The value of the balancing parameter C is determined through numerical experiment. Even though C is undetermined, once it is determined, it should be a constant for a certain discretization scheme. Equation (17) is prescribed heuristically here with no rigorous derivation. However, detailed numerical verification of the performance of the given artificial diffusion coefficient by Eq. (17) is conducted in the next section.

Practical implementation of Eq. (17) requires knowledge of the local angular and spatial scales. Two angular discretization schemes are considered in this article, the S_N scheme and the PCA scheme [22, 23]. By noticing the scale characteristics of quadrature weight, the local angular scale of direction $\mathbf{\Omega}^m$ is defined as

$$h_a^m = h_a(\mathbf{\Omega}^m) = w^m \tag{18}$$

For the spectral or finite-element method, the local spatial length scale at node j is defined as

$$h_{s,j} = h_s(\mathbf{r}_j) = \sqrt[d]{\tilde{w}_j}, \qquad \tilde{w}_j = \int_V \phi_j(\mathbf{r})\, dV \tag{19}$$

where d denotes spatial dimension and $\tilde{w}_j$ can be considered a virtual volume around node j. It is noted that the sum of w_j through each node equals the volume of the solution domain.

Combining the definition of local angular scale, local spatial scale, and artificial diffusion coefficient, namely, Eqs. (18), (19), and (17), the discretization-based

on artificial diffusion given by Eq. (12*a*) can be written as

$$K_{ji}^{m} = \int_V (\mathbf{\Omega}^m \cdot \nabla\phi_i + \beta\phi_i)\phi_j \, dV + [Ch_a^m + (1 - C)h_{s,j}^{p+1}] \int_V \nabla\phi_i \cdot \nabla\phi_j \, dV \qquad (20)$$

which gives the final discretization of the adaptive isotropically artificial diffusion scheme (AISO). The streamwise artificial diffusion can also be adaptively applied in this way.

RESULTS AND DISCUSSION

The aforementioned methods are implemented using the procedure presented in [10], which uses a global iteration as in the DOM to update the source term. The matrix equation for each direction given by Eq. (8) is solved by Gaussian elimination. The maximum relative error 10^{-4} of incident radiation ($|G_{\text{new}} - G_{\text{old}}|/G_{\text{new}}$) is taken as the stop criterion for the global iteration. To verify the formulations presented in this article, four test cases are selected to verify the performance of the methods presented.

Case 1: Radiative Equilibrium in a Square Enclosure Filled with Nonscattering Media

We consider a radiative equilibrium problem in a black square enclosure filled with nonscattering media. The optical thickness based on the side length L of the square is $\tau_L = \beta L = 1.0$. The temperature of the bottom wall (T_{w1}) is 1,000 K, and the other walls are kept at 500 K. This problem was also studied by Larsen and Howell [24] using the zone method. As shown in Figure 1, the incident radiation energy of a node P in the interior of the enclosure comes from two regions, namely,

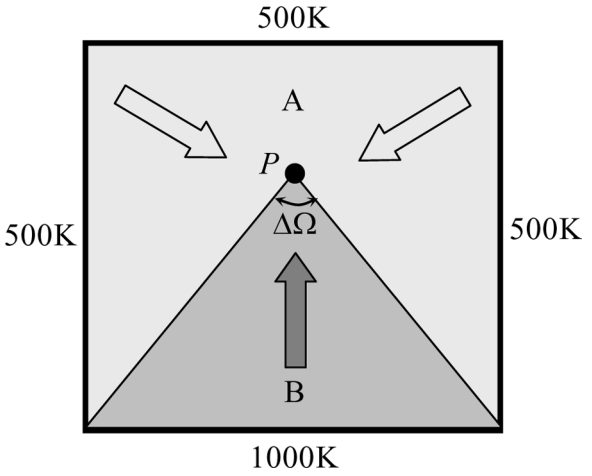

Figure 1. Schematic of boundary loading-induced discontinuity of angular distribution of radiative intensity.

regions A and B. The radiative energy coming from region B is stronger than that coming from region A. This results in discontinuities of radiative intensity of node P in solid angular space. Inaccuracy of the angular discretization scheme will cause "wiggles" in the numerical results of the RTE, which is known as the ray effect [12, 16, 17]. It should be noted that two kinds of error exist in the numerical solution of the RTE, namely, the ray effects and false scattering, and these errors interact with each other.

The spectral element method with different artificial diffusion schemes is applied to solve the temperature distribution along the vertical symmetry line ($x/L = 0.5$) of the enclosure. The result of the zone method [24] is taken as benchmark for comparison. Two spatial decomposition schemes shown in Figures 2*a* and 2*b*, namely, (*a*) 36 elements with second-order polynomial approximation and (*b*) 4 elements with eighth-order polynomial approximation, are used to test the performance of the stabilization schemes on low- and high-order approximations, respectively. The solid angular space is discretized by an S_6 scheme.

To study the performance of different artificial diffusion schemes in the SEM with low-order approximation, Figures 3*a* and 3*b* shows the relative error distribution of temperature along the vertical symmetry line ($x/L = 0.5$) obtained by the SEM with different artificial diffusion schemes on mesh (*a*). With increasing of α from 0.01 to 0.1, the diffusion is effectively enhanced and the stability performance of the streamwise artificial diffusion schemes, namely, SU, SUPG, and GLS, improved a little. Because of the inconsistency of the ISO scheme, a large α reduces its performance, even though a better choice of α, namely, $\alpha = 0.01$, gives very good results as compared to others. To further study the performance of different artificial diffusion schemes on the SEM with high-order approximation, Figures 4*a* and 4*b* show the relative error distribution of temperature along the vertical symmetry line ($x/L = 0.5$) obtained by the SEM with different artificial diffusion schemes on mesh (*b*). In this case, with the increasing of α from 0.01 to 0.1, all the streamwise artificial diffusion schemes, namely, SU, SUPG, and GLS, do not show improvement in stability. The pattern of error distribution of these streamwise artificial diffusion schemes resembles that of the LS scheme. However, the ISO scheme shows very good performance compared to the streamwise artificial diffusion schemes.

By comparison, the ISO scheme shows a different pattern than the streamwise artificial diffusion schemes and gives better performance in the cases of both low-order and high-order approximation used in the SEM. For this reason, the following study is focuses on the improved version of the ISO scheme with adaptive choice of artificial diffusion coefficient as presented in this article, namely, the AISO scheme.

Case 2: Square Enclosure Filled with Isotropically Scattering Media

In this case, the radiative transfer in a black square enclosure filled with isotropically scattering media with single scattering albedo $\omega = 1.0$ is considered. The optical thickness based on the side length L of the square is $\tau_L = 1.0$. The temperature of the bottom wall is kept at $T_{w1} = 1,000\,\mathrm{K}$, but all other walls and the media are kept cold (0 K). Similar to what is depicted in Figure 1, because of the discontinuity or large gradient of boundary loading, there is a large angular nonuniformity of radiative intensity, thus it is very difficult to accurately integrate the angular

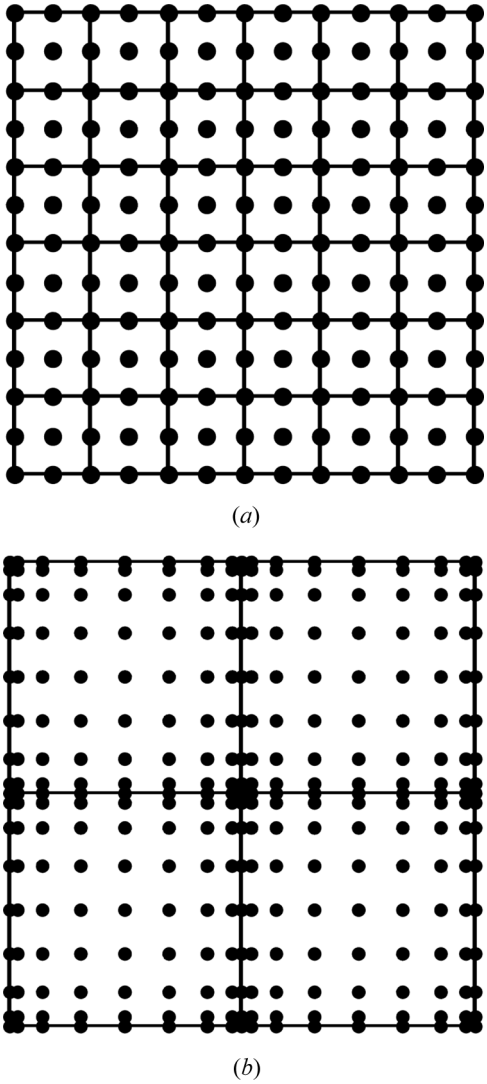

Figure 2. Mesh decomposition and spectral node distribution: (*a*) 36 elements with second-order polynomial approximation; (*b*) 4 elements with eighth-order polynomial approximation.

distribution of radiative intensity by the discrete-ordinates approach. This case was studied by several researchers [11, 16, 24, 25] and serves as a good test case for verifying the performance of the numerical method.

The SEM with AISO scheme (AISO-SEM) is applied to solve the radiative heat flux distribution along the top wall. First the balancing parameter C is determined from numerical experiment. Figure 5 shows the results obtained by the AISO-SEM under different values of C, namely, $C = 0.01$, 0.05, and 0.25. Here the square enclosure is uniformly decomposed into 9 elements and fourth-order polynomial approximation is used, the angular discretization taking S_8. It can be seen that very

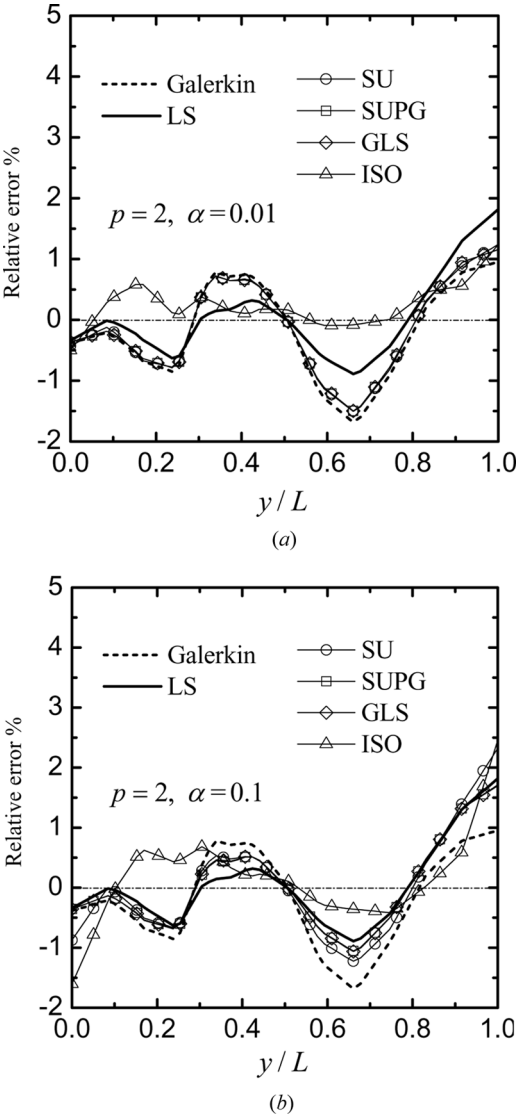

Figure 3. Relative error distribution of temperature along the centerline obtained by the SEM with different artificial diffusion schemes under low-order approximation $p = 2$: (*a*) $\alpha = 0.01$; (*b*) $\alpha = 0.1$.

small values of C result in poor stability, while very large values of C result in large false scattering. In this test case, taking the value of C as 0.05 works very well. In the following analysis, C is taken as 0.05 for more general verification.

Figures 6*a*–6*c* show the radiative heat flux distribution along the top wall of the square enclosure obtained by standard Galerkin SEM (GSEM), least-square SEM (LSSEM), and the AISO-SEM under the same spatial and angular discretizations, respectively, and compared to the quasi-exact solution of Crosbie

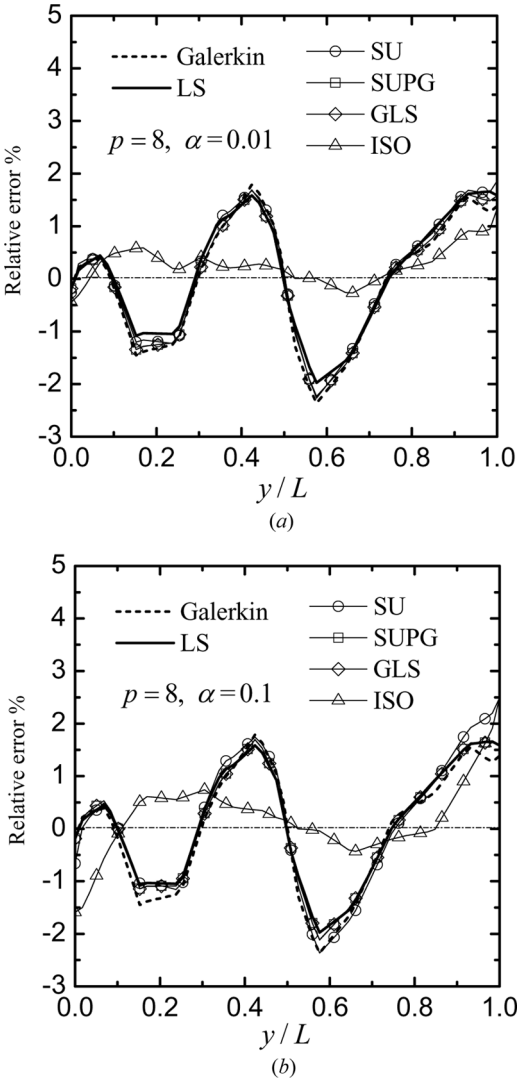

Figure 4. Relative error distribution of temperature along the centerline obtained by the SEM with different artificial diffusion schemes under low-order approximation $p = 8$: (*a*) $\alpha = 0.01$; (*b*) $\alpha = 0.1$.

and Schrenker [25]. The spatial discretization uses 9 uniform quadrilateral elements and fourth-order polynomial approximation. Four angular discretization scheme are used to better show the ray effects of the method, namely, S_4, S_6, S_8, and the PCA scheme with $N_\theta \times N_\varphi = 20 \times 40$. There are obvious "wiggles" in the results obtained using the GSEM and the LSSEM, though they are much mitigated with refinement of angular discretization. The results obtained using the AISO-SEM are free of "wiggles" under different accuracies of angular discretization and show very good performance, which demonstrates that the AISO scheme can effectively mitigate the ray effects encountered in the solution of this problem.

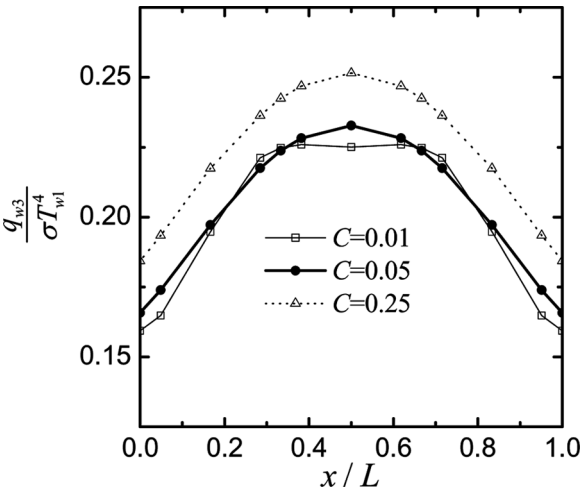

Figure 5. Dimensionless radiative heat flux distribution along the top wall of the square enclosure obtained by the SEM with AISO scheme under different values of C.

Figure 7 shows the radiative heat flux distribution along the top wall of the square enclosure obtained using the AISO-SEM under five different spatial decompositions, namely, $M \times p = 12 \times 1$, 6×2, 3×4, and 2×6. Here, the square enclosure is decomposed uniformly into quadrilateral elements and the spatial decompositions are denoted as $M \times p$, where M is the number of elements per side of the square enclosure and p is the order of polynomial approximation. In this notation, the total number of elements is $N_{\text{el}} = M \times M$ and the total number of solution nodes is $N_{\text{sol}} = (M \times p + 1)^2$. The selected spatial decomposition schemes have the same number of solution nodes. The angular discretization takes the PCA scheme with $N_\theta \times N_\varphi = 20 \times 40$. It is seen that with increasing of order of polynomial approximation, the accuracy of the result obtained by the AISO-SEM increases rapidly compared to the reference result and no "wiggles" exist in the solutions, which demonstrates that the AISO-SEM is robust in both low- and high-order polynomial approximation, and higher-order approximation gives better accuracy under the same number of computational efforts. The AISO scheme does not degrade much the accuracy of higher-order approximation.

Case 3: Quadrilateral Enclosure with a Curved Bottom Wall

To verify the performance of the AISO-SEM in solving a problem with complex geometry, the radiative transfer in a quadrilateral enclosure with a curved bottom wall is studied. The configuration of the geometry is shown in Figure 8. The enclosure is filled with isotropically scattering media with scattering albedo of $\omega = 1.0$. The optical thickness based on the width R of the top wall is $\tau_L = \beta R = 1.0$. The curved bottom wall is kept hot (1,000 K), while all other walls and the media are kept cold (0 K). This case was also studied by Parthasarathy

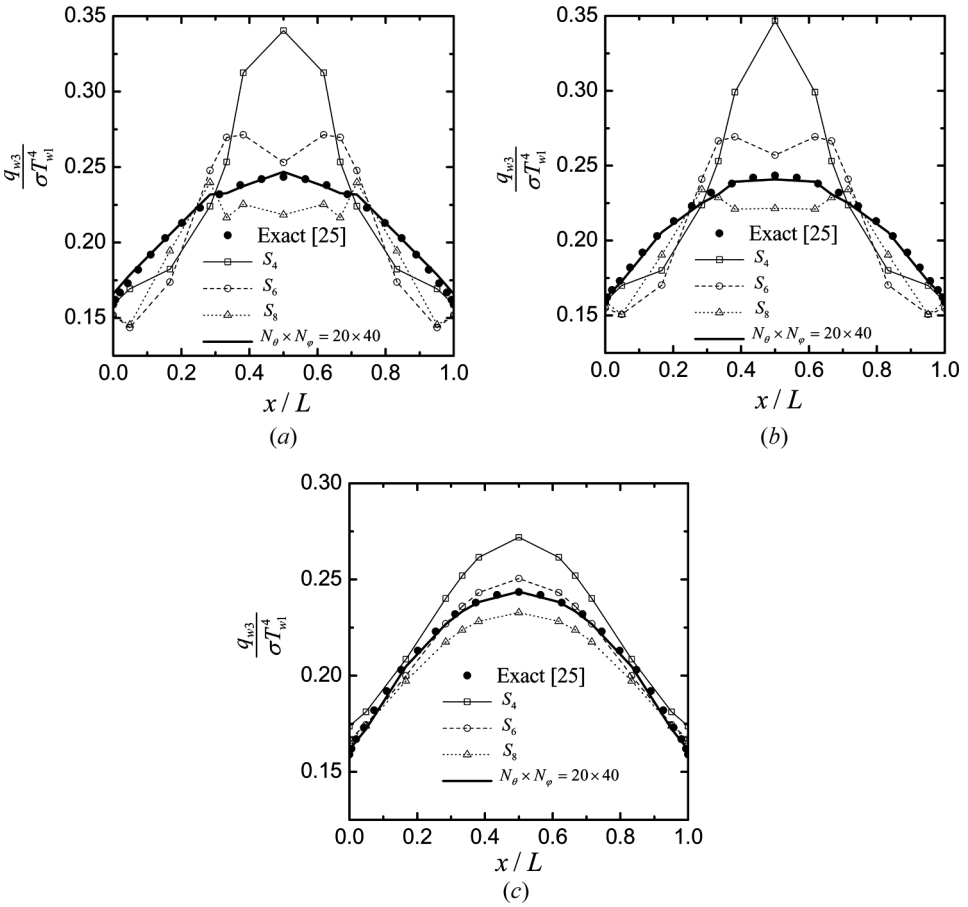

Figure 6. Dimensionless radiative heat flux distribution along the top wall of the square enclosure obtained by: (*a*) GSEM; (*b*) LSSEM; (*c*) AISO-SEM under the same spatial and different angular discretizations.

et al. [26] and by Sakami and Charette [27]. The AISO-SEM is applied to solve the dimensionless radiative heat flux along the top wall. The enclosure is decomposed into 255 quadrilateral elements as shown in Figure 8. The results obtained using the AISO-SEM with different orders of approximation for spatial discretization and different angular discretization schemes are shown in Figure 9, and are compared to the result obtained by Parthasarathy et al. [26] using the Monte Carlo method. It can be seen that the result obtained using the AISO-SEM is stable and free of "wiggles" for all spatial and angular discretization schemes. With increasing order p of polynomial approximation of spatial discretization, the solution accuracy is considerably improved for both angular discretization, namely, S_8 and the PCA scheme with $N_\theta \times N_\varphi = 20 \times 40$. This demonstrates that the SEM based on the AISO scheme is stable and effective in solving radiative transfer in complex geometry.

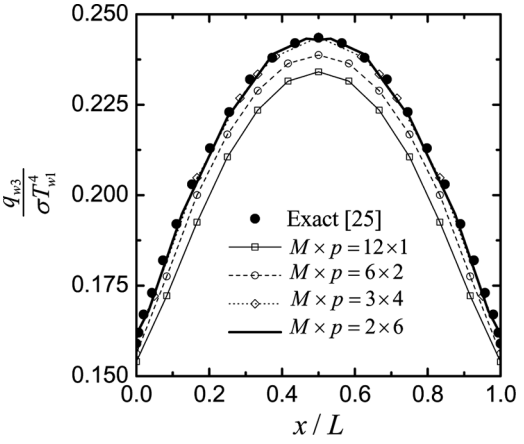

Figure 7. Dimensionless radiative heat flux distribution along the top wall of the square enclosure obtained by the AISO-SEM under five different spatial decomposition schemes.

Case 4: Semicircular Enclosure with a Circular Hole

As a further verification, we consider the radiative transfer in a semicircular enclosure with a circular hole filled with nonscattering media as shown in Figure 10. The medium is kept hot (1,000 K), while all other walls are black and kept cold (0 K). In this case, the circular hole plays a role as an obstacle. The shielding effect of the obstacle will cause discontinuity in angular distribution of radiative intensity, which makes it difficult to do angular integration efficiently and accurately. As discussed and demonstrated in [11], ray effects are encountered in this case when it is solved by the GSEM.

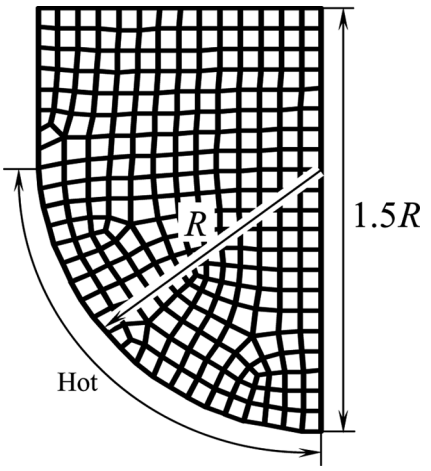

Figure 8. Configuration and mesh decomposition of the irregular quadrilateral enclosure.

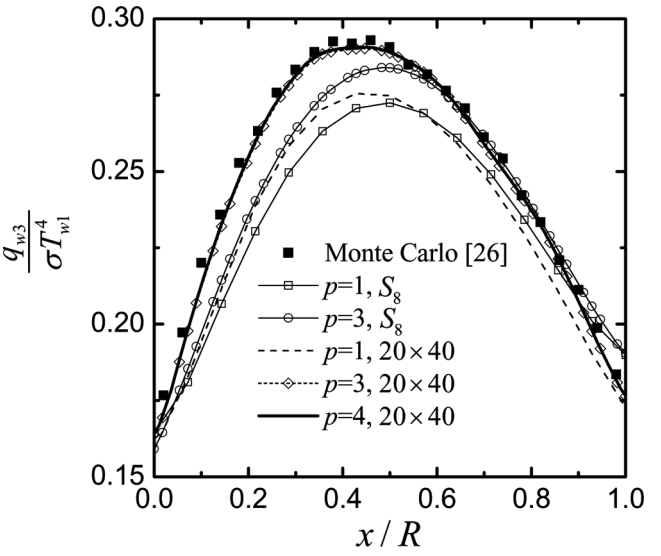

Figure 9. Dimensionless radiative heat flux distribution along the top wall of the irregular quadrilateral enclosure.

The AISO-SEM is applied to solve the radiative heat flux along the bottom wall of the enclosure. The enclosure is decomposed into 272 quadrilateral elements as shown in Figure 10. Figures 11*a* and 11*b* show the results obtained using the AISO-SEM with third-order polynomial approximation and different angular discretization schemes for two values of optical thickness, namely, $\tau_L = \beta R = 0.1$ and 1.0, respectively. The exact solution obtained by Kim et al. [28] is taken here as a benchmark. The result obtained using the GSEM under the same spatial discretization is also shown for comparison. It is found that obvious "wiggles" exists in the results obtained using the GSEM. However, the result obtained using the AISO-SEM is free of "wiggles" even in a case of very coarse angular discretization, such as $N_\theta \times N_\varphi = 5 \times 10$. With refinement of angular discretization from

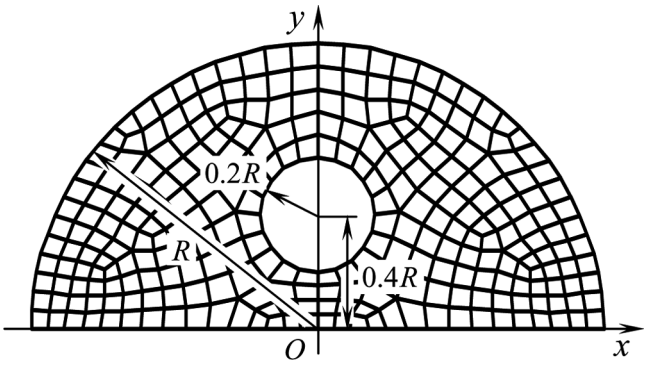

Figure 10. Configuration and mesh decomposition of the semicircular enclosure.

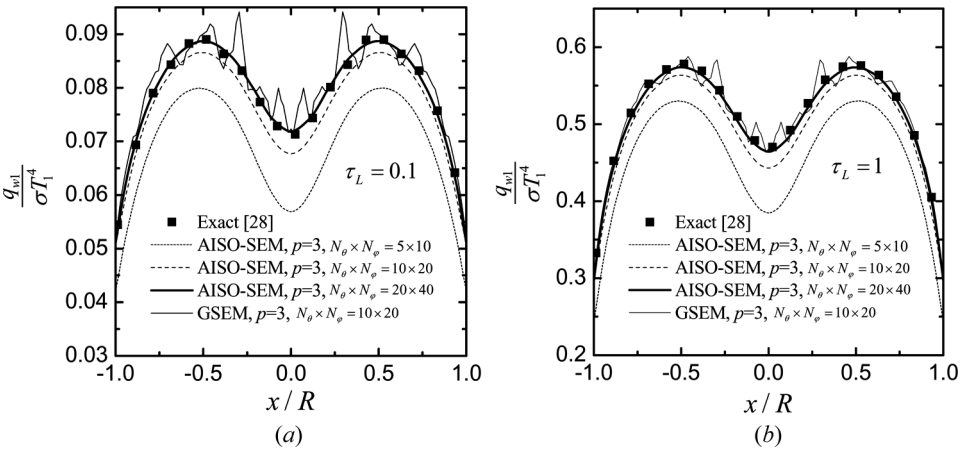

Figure 11. Dimensionless net radiative heat flux distribution along the bottom wall of the semicircle enclosure: (*a*) $\tau_L = 0.01$; (*b*) $\tau_L = 0.01$.

$N_\theta \times N_\varphi = 5 \times 10$ to 20×40, the result of the AISO-SEM stably approaches the exact result for different values of optical thickness. Though the cause of this kind of ray effects is different than in the cases discussed formerly, the AISO-SEM is demonstrated to be very robust to solve this kind of problem.

CONCLUSIONS

Ray effects and false scattering are two major drawbacks of the methods based on discretization of the radiative transfer equation. As for the high-order spectral element methods, the ray effects become dominant. An AISO scheme has been developed for the spectral or finite-element method to mitigate the ray effects encountered in the solution of radiative transfer problems. The artificial diffusion coefficient is determined heuristically from both local angular discretization scale and local spatial discretization scale. The scheme is easily and efficiently implemented under the spectral or finite-element method framework. The isotropically artificial diffusion scheme shows very good performance in mitigating the "wiggles" in both low- and high-order spatial approximation. The SEM based on the AISO scheme is stable and effective for solving radiative transfer in simple and complex geometries, and is also robust in mitigating ray effects of different origins.

REFERENCES

1. W. A. Fiveland, Three-Dimensional Radiative Heat-Transfer Solutions by the Discrete-Ordinates Method, *J. Thermophys. Heat Transfer*, vol. 2, pp. 309–316, 1988.
2. G. D. Raithby and E. H. Chui, A Finite-Volume Method for Predicting a Radiant Heat Transfer in Enclosures with Participating Media, *ASME J. Heat Transfer*, vol. 112, pp. 415–423, 1990.
3. J. C. Chai and H. S. Lee, Finite-Volume Method for Radiation Heat Transfer, *J. Thermophys. Heat Transfer*, vol. 8, pp. 419–425, 1994.

4. J. Y. Murthy and S. R. Mathur, Finite Volume Method for Radiative Heat Transfer Using Unstructured Meshes, *J. Thermophys. Heat Transfer*, vol. 12, pp. 313–321, 1998.
5. V. B. Kisslelev, L. Roberti, and G. Perona, An Application of the Finite-Element Method to the Solution of the Radiative Transfer Equation, *J. Quant. Spectrosc. Radiat. Transfer*, vol. 51, pp. 603–614, 1994.
6. L. H. Liu, Finite Element Simulation of Radiative Heat Transfer in Absorbing and Scattering Media, *J. Thermophys. Heat Transfer*, vol. 18, pp. 555–557, 2004.
7. X. Cui and B. Q. Li, Discontinuous Finite Element Solution of 2-D Radiative Transfer with and without Axisymmetry, *J. Quant. Spectrosc. Radiat. Transfer*, vol. 96, pp. 383–407, 2005.
8. L. H. Liu and L. J. Liu, Discontinuous Finite Element Method for Radiative Heat Transfer in Semitransparent Graded Index Media, *J. Quant. Spectrosc. Radiat. Transfer*, vol. 105, pp. 377–387, 2007.
9. J. P. Pontaza and J. N. Reddy, Least-Squares Finite Element Formulations for One-Dimensional Radiative Transfer, *J. Quant. Spectrosc. Radiat. Transfer*, vol. 95, pp. 387–406, 2005.
10. J. M. Zhao and L. H. Liu, Least-Squares Spectral Element Method for Radiative Heat Transfer in Semitransparent Media, *Numer. Heat Transfer B*, vol. 50, pp. 473–489, 2006.
11. J. M. Zhao and L. H. Liu, Discontinuous Spectral Element Method for Solving Radiative Heat Transfer in Multidimensional Semitransparent Media, *J. Quant. Spectrosc. Radiat. Transfer*, vol. 107, pp. 1–16, 2007.
12. J. C. Chai, H. S. Lee and S. V. Patankar, Ray Effects and False Scattering in the Discrete Ordinates Method, *Numer. Heat Transfer B*, vol. 24, pp. 373–389, 1993.
13. P. J. Coelho, The Role of Ray Effects and False Scattering on the Accuracy of the Standard and Modified Discrete Ordinates Methods, *J. Quant. Spectrosc. Radiat. Transfer*, vol. 73, pp. 231–238, 2002.
14. H. S. Li and G. Flamant, Reduction of False Scattering of the Discrete Ordinates Method, *J. Heat Transfer*, vol. 124, pp. 837–844, 2002.
15. H. P. Tan, H. C. Zhang, and B. Zhen, Estimation of Ray Effects and False Scattering in Approximate Solution Method for Thermal Radiative Transfer Equation, *Numer. Heat Transfer A*, vol. 46, pp. 807–829, 2004.
16. M. A. Ramankutty and A. L. Crosbie, Modified Discrete Ordinates Solution of Radiative Transfer in Two-Dimensional Rectangular Enclosures, *J. Quant. Spectrosc. Radiat. Transfer*, vol. 57, pp. 107–140, 1997.
17. P. J. Coelho, A Modified Version of the Discrete Ordinates Method for Radiative Heat Transfer Modelling, *Comput. Mech.*, vol. 33, pp. 375–388, 2004.
18. J. M. Zhao and L. H. Liu, Second Order Radiative Transfer Equation and Its Properties of Numerical Solution Using Finite Element Method, *Numer. Heat Transfer B*, vol. 51, pp. 391–409, 2007.
19. J. C. Chai, H. S. Lee, and S. V. Patankar, Finite-Volume Method for Radiation Heat Transfer, in W. J. Minkowycz and E. M. Sparrow (eds.), *Advances in Numerical Heat Transfer*, pp. 109–141, Taylor & Francis, New York, 2000.
20. A. N. Brooks and T. J. R. Hughes, Streamline Upwind/Petrov-Galerkin Formulations for Convection Dominated Flows with Special Emphasis on the Incompressible Navier-Stokes Equations, *Comput. Meth. Appl. Mech. Eng.*, vol. 32, pp. 199–259, 1982.
21. C. Johnson, *Numerical Solutions of Partial Differential Equations by the Finite Element Method*, Cambridge University Press, New York, 1987.
22. L. H. Liu, L. Zhang, and H. P. Tan, Finite Element Method for Radiation Heat Transfer in Multi-dimensional Graded Index Media, *J. Quant. Spectrosc. Radiat. Transfer*, vol. 97, pp. 436–445, 2006.

23. J. M. Zhao and L. H. Liu, Solution of Radiative Heat Transfer in Graded Index Media by Least Square Spectral Element Method, *Int. J. Heat Mass Transfer*, vol. 50, pp. 2634–2642, 2007.
24. M. E. Larsen and J. R. Howell, The Exchange Factor Method: An Alternative Zonal Formulation of Radiating Enclosure Analysis, *J. Heat Transfer*, vol. 107, pp. 936–942, 1985.
25. A. L. Crosbie and R. G. Schrenker, Radiative Transfer in a Two-Dimensional Rectangular Media Exposed to Diffuse Radiation, *J. Quant. Spectrosc. Radiat. Transfer*, vol. 31, pp. 339–372, 1984.
26. G. Parthasarathy, S. V. Patankar, J. C. Chai, and H. S. Lee, Monte Carlo Solutions for Radiative Heat Transfer in Irregular Two-Dimensional Geometries, *ASME HTD*, vol. 276, pp. 191–201, 1994.
27. M. Sakami and A. Charette, Application of a Modified Discrete Ordinates Method to Two-Dimensional Enclosures of Irregular Geometry, *J. Quant. Spectrosc. Radiat. Transfer*, vol. 64, pp. 275–298, 2000.
28. M. Y. Kim, S. W. Baek, and J. H. Park, Unstructured Finite-Volume Method for Radiative Heat Transfer in a Complex Two-Dimensional Geometry with Obstacles, *Numer. Heat Transfer B*, vol. 39, pp. 617–635, 2001.